Identifying Glaucomatous Damage to the Macula

Muhammed S. Alluwimi, PhD,* William H. Swanson, PhD, FAAO, and Brett J. King, OD, FAAO

SIGNIFICANCE: Measurements of the macula have been increasingly used to diagnose and manage patients with glaucoma. Asymmetry analysis was clinically introduced to assess damage to the macular ganglion cells in patients with glaucoma, but its effectiveness is limited by high normal between-subject variability.

PURPOSE: We aimed to reduce the high normal between-subject variability and improve the potential of asymmetry analysis to identify glaucomatous damage to the macula.

METHODS: Twenty patients with glaucoma (aged 57 to 85 years) and 30 age-similar control subjects (aged 53 to 89 years) were recruited from a longitudinal glaucoma study. Participants were imaged with the Spectralis OCT using the posterior pole protocol; measurements of the averaged retinal thickness and ganglion cell layer (GCL) thickness were obtained. We established three zones per hemifield within the central ±9°, based on the lowest between-subject variability that we previously found and the course of retinal nerve fiber layer projections. The criteria for flagging abnormality were at least two contiguous zones when $P < 5\%$ or one zone when $P < 1\%$ with two-tailed tests.

RESULTS: Between-subject variability of the asymmetry analysis for both retinal and GCL thicknesses remained lower than that of the average thickness across each zone in control subjects ($F > 2.52$, $P < .01$). Asymmetry analysis of retinal and GCL thicknesses flagged 16 and 18 of 20 patients, respectively.

CONCLUSIONS: Between-subject variability was reduced in control subjects using the three zones; our criteria identified glaucomatous damage to the macula in most of the patients. We used high-density B-scans to confirm the patterns of the glaucomatous damage we found in this study.

Optom Vis Sci 2018;95:96–105. doi:10.1097/OPX.0000000000001166

OPEN

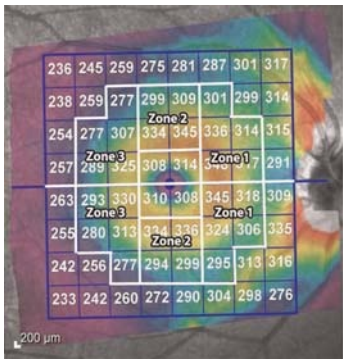

Author Affiliations:
Indiana University School of Optometry, Bloomington, Indiana
*malluwim@indiana.edu
Present Address:
Qassim University, College of Applied Medical Sciences, Department of Optometry, Buraidah City
Saudi Arabia, 52571

Glaucoma is a group of chronic, progressive neuropathies that cause morphological changes to the optic nerve head and retinal nerve fiber layer that are associated with visual field defects. It had been widely believed that glaucomatous damage starts in the peripheral visual field and continues to central fixation at the advanced stages of the disease. In that regard, the central 24-2 visual field grid has been the standard for automated perimetry testing in patients with glaucoma.

The 24-2 grid is used to sample 54 field locations across the central 30° of the retina; 6° separate each two points of the grid in the vertical and horizontal directions. This grid contains only four perimetric locations that sample the central ±8°, which we defined in the current study as the macula. Therefore, glaucomatous damage to the macula is poorly sampled by the 24-2 grid or larger grids. In advanced stages of the disease, the 10-2 grid is usually applied where 68 locations, with 2° separation, are tested across ±10° from the fovea.

The evaluation of damage to macula will help assess central vision in patients with glaucoma, loss of which affects the quality of life.[1] Glaucomatous damage to the macula has been recognized to be more common in patients with glaucoma than it had been previously thought. Several studies suggested that glaucomatous visual field defects could involve the macula at early stages of glaucoma,[2–5] but these studies did not provide structural data supporting their findings. The lack of corresponding structural data led to a minimal impact of these studies on clinical practice. Structural data may help clinicians build their decision of whether 10-2 testing is essential, in addition to 24-2 testing. Such a patient may have subtle damage at the macula that has been missed by the 24-2 grid, and that patient may continue losing ganglion cells without appropriate diagnosis and management.

In the late 1990s, several studies started reporting that structural damage to the macula in patients with glaucoma is more common than it was previously thought. Zeimer et al.[6–8] and Asrani et al.[9] first attempted to measure the retinal thickness at the macula and emphasized the potential of measuring macular thickness and its asymmetry between the superior and inferior portions in patients with glaucoma. Other studies investigated the importance of macular measurements to detect glaucomatous damage by applying the asymmetry between the superior and inferior hemifields of the macular region as measured by optical coherence tomography, but corresponding functional data from the 10-2 grid were not provided.[10,11] A comparison between macular thickness measurements with optical coherence tomography and perimetric data using the 10-2 grid was presented by Kanadani et al.[12] in patients with glaucoma in which they used the Humphrey field analyzer and multifocal visual evoked potential for the functional measurements.

With advances in imaging technologies, manual[13] and automated segmentations[14–16] of the ganglion cell layer and inner plexiform layer in the macula were then introduced. Studies demonstrated measured ganglion cell layer and inner plexiform layer

data and corresponding functional glaucomatous defects using 10-2 locations. However, there was a significant amount of overlap between the measured thicknesses of the ganglion cell layer and inner plexiform layer in patients with glaucoma and control participants. The inclusion of inner plexiform layer may reduce the ability to detect reduction in the ganglion cell layer in patients with glaucoma. Although ganglion cell layer was separated from inner plexiform layer (IPL) in another study, there was still substantial overlap between the patient and control data.[17]

More recently, posterior pole asymmetry analysis was introduced to the clinic with the Spectralis optical coherence tomograph (V 5.4; Heidelberg Engineering, Heidelberg, Germany).[18] This protocol provides measurements of retinal thickness for a 64-box grid superimposed on a 30° × 25° region of the macula. It had been demonstrated that black boxes of the grid (that indicate the extreme values of the asymmetry analysis) could be found in healthy subjects, which may mislead the interpretation of the printouts. Um et al[19] proposed using five zones that cover most of the posterior pole grid and mimic the glaucoma hemifield test. In a previous study from our laboratory,[20] we demonstrated that there was high normal between-subject variability of the asymmetry analysis in the peripheral regions of the grid, and this variation could be reduced using the asymmetry analysis. However, our study was limited by using retinal thickness measurements without segmenting out the ganglion cell layer and retinal nerve fiber layer, the most affected layers in patients with glaucoma.

In this study, our goal was to apply the asymmetry analysis in a subset of the posterior pole grid boxes based on the trajectory of the retinal nerve fiber layer, the clinical knowledge of the patterns of glaucomatous damage within the macula, and the regions that we found in our previous study[20] to have low variability of the asymmetry analysis. We aimed to improve the interpretation of the asymmetry analysis to provide better assessment of macular damage in patients with glaucoma.

METHODS

Participants

Twenty patients with primary open-angle glaucoma (mean and SD of 72 ± 7 years, aged 57 to 85 years) and right eyes of 30 age-similar control participants (mean and SD of 70 ± 9 years, aged 53 to 89 years) were selected from an ongoing glaucoma study at Indiana University Bloomington. Demographic and perimetric data are given in Table 1. The study definition of glaucoma is given elsewhere.[21] This research followed the tenets of the Declaration of Helsinki. Informed consent was obtained from the subjects after explanation of the nature and possible consequences of the study. This research was approved by the institutional review board at Indiana University.

TABLE 1. Descriptive statistics (median and range) for demographic and perimetric data for control participants and patients with glaucoma

Parameter	Control participants (n = 30)	Patients with glaucoma (n = 20)
Age (y)	70 (53–89)	74 (57–85)
Sex		
Male	13 (43.3%)	11 (55.0%)
Female	17 (56.7%)	9 (45.0%)
Mean deviation (dB)	0.2 (–1.9 to +1.6)	–5.1 (–17.0 to +1.4)
Pattern SD (dB)	1.7 (1.2–3.6)	7.6 (1.7–14.1)

Basic inclusion criteria were comprehensive eye examination within the last 4 years, best corrected visual acuity of 20/20 (for subjects >70 years old, this criterion was set to 20/25 visual acuity), spherical equivalent from +3.0 to –6.0 diopters (D), and absence of ocular disease (other than glaucoma in the patient group) such as diabetic retinopathy, degenerative myopia, macular degeneration, and prior vein occlusion. Inclusion criteria also included reliable perimetric data using the 24-2 pattern (<15% false positive, <20% fixation losses). Additional inclusion criteria for the age-similar control subjects were visual field within normal limits and open anterior chamber angle, and an additional exclusion criterion was intraocular pressure greater than 21 mmHg for two or more clinical visits. An additional exclusion criterion for patients was intraocular pressure of 30 mmHg or greater on a recent clinic visit.

Common exclusion criteria were a history of ocular disease or surgery (except for those with uncomplicated cataract surgery and glaucoma in the patient group) and optical coherence tomography images that had quality of less than 20.

Imaging

A Spectralis optical coherence tomograph was used to image the macular region using the posterior pole protocol. For this protocol, the Spectralis provides 61 horizontal B-scans across the macular region, 120 μm apart, with axial resolution of 7 μm and lateral resolution of 14 μm. Then, a 64-box grid was overlaid on the central 24° × 24° of the retinal region. Each box of this grid is 3° × 3° and represents the average of measured retinal thickness. One of the authors (MSA) realigned and centered the grid on the fovea and rotated the central line of this grid to the same direction as the foveal-disc angle. The Spectralis automatically segmented the B-scans from the inner limiting membrane to Bruch membrane. The operator had to correct segmentation errors with the macular scans for two control participants. B-scans were reviewed for both patients with glaucoma and control participants to confirm that there was no retinal disease affecting the retinal thickness, except the reduction in the thickness of retinal nerve fiber layer, ganglion cell layer, and inner plexiform layer as a result of the glaucomatous damage.

Optical Coherence Tomography En Face Images

To confirm damage identified by the asymmetry analysis of the retinal thickness and ganglion cell layer thickness, en face images were gathered using Spectralis optical coherence tomography. En face images of the retinal nerve fiber layer images allow evaluation of the retinal nerve fiber layer bundles through a full range of depths below the inner limiting membrane. We used dense vertical B-scans, separated by 30 μm, comprising four different rectangles. The width and height of the first rectangle were 25° × 20°, and the temporal fixation target was used so that the operator placed the rectangle temporal to the fovea. The second and third scans were each designed to cover a retinal area of 10° × 20°, to image superior and inferior macular regions by using fixation targets above and below the fovea. The fourth scan covered a 15° × 30° rectangle centered on the optic disc, using the nasal fixation target. We applied this protocol to obtain en face retinal nerve fiber layer images corresponding to much of the visual field area tested within the central 30° of the retina.

The volume scans were exported from the Spectralis optical coherence tomograph and read by a custom Matlab (The Mathworks Inc., Natick, MA) program, which was developed by our laboratory. This custom program was used to montage volume scans for different regions of the retina into a single volume scan and provided en face images at different depths from the inner limiting membrane.

New Zones and Criteria

Three zones were developed within the posterior pole grid based on regions with low between-subject variability that we found in our previous study,[20] in which normative data were collected from a homogenous group of young healthy control participants (Fig. 1). These three zones were designed by following patterns of the retinal nerve fiber layer bundles around the fovea and by including few and smaller blood vessels than those in the peripheral regions of the 64-box grid. We included the area of ±9° (from the foveola) in these zones where the highest density and low between-subject variability were reported in a histological study of the ganglion cell distribution in control participants.[22] Of the 64-box grid, zone 1 included boxes that covered a region from the fovea to ~9° nasal to the fovea. Zone 2 covered boxes ~9° above (or below) the fovea. The third zone included boxes extending from the fovea toward the region of the temporal raphe. Four boxes around the foveola were excluded to reduce the effect of abrupt reduction in thickness.

To assess whether the reduction of between-subject variability was maintained with the new zones, the normative data in our previous study[20] were reanalyzed. The asymmetry was calculated as the difference between the average of measured retinal thickness of the superior zones and the corresponding inferior zones. The SD of the asymmetry and retinal thickness were compared using three F tests. The significance level was set at $P < .017$ after we applied a Bonferroni correction.

To analyze the data, we created plots that included 28 boxes of the grid (from the superior and inferior new zones) from 30 age-similar control participants recruited in our previous study. Data for within-eye asymmetry from age-similar control participants were used to compute the reference range, when $P = .05$ and $P = .01$ are set at 1.96 and 2.64 SDs from mean normal with two-tailed tests, assuming a Gaussian distribution. Criteria for abnormality were set for within-eye asymmetry: two contiguous zones when $P < 5\%$ or one zone when $P < 1\%$. Plots for patients were then created to visualize the reduction in retinal thickness as compared with our normative data from the age-similar control participants.

To assess the potential of the asymmetry analysis for the measured ganglion cell layer, we applied a new autosegmentation tool provided by the Spectralis optical coherence tomograph, which segmented individual retinal layers from the inner limiting membrane to Bruch membrane. Then, the posterior pole grid was applied to the autosegmented ganglion cell layer thickness measurements; the average ganglion cell layer thickness was shown for each box of the grid. The new zones and criteria used for the retinal thickness in this study were applied to the ganglion cell layer measurements. The goal of this analysis was to evaluate the interpretation of the new zones and develop criteria to identify glaucomatous damage to the macula, using the segmented ganglion cell layer thickness instead of using the whole measured retinal thickness.

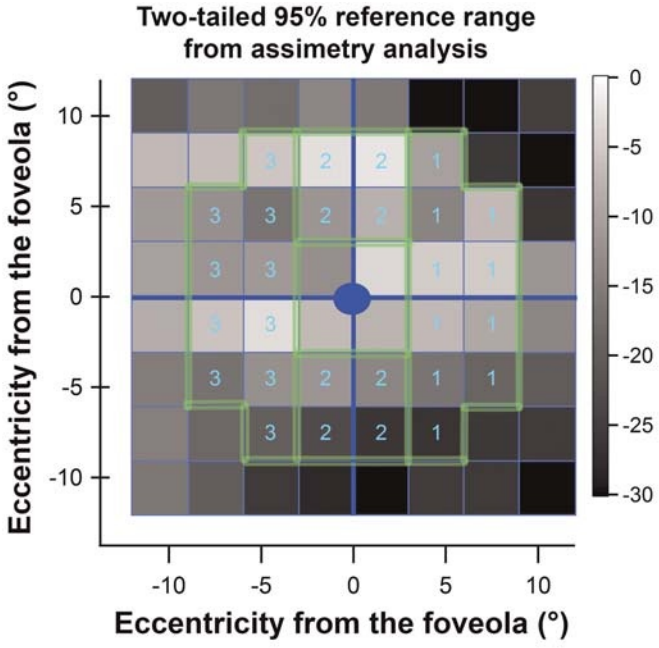

FIGURE 1. A gray-scale map of between-subject variability of asymmetry for right eyes of 33 young healthy control subjects as previously published. This grid mimics the Spectralis OCT printouts; the gray scale of each box in this grid represents the two-tailed 2.5th percentile reference limits of the within-eye asymmetry. The green lines demarcate the three zones that we applied in this study where regions of low between-subject variability were included.

RESULTS

Asymmetry Analysis of the Retinal Thickness

Means ± SDs of the retinal thickness for the age-similar control participants were as follows: 314 ± 12 µm for zone 1, 309 ± 9 µm for zone 2, and 289 ± 10 µm for zone 3. The confidence interval of SDs for the retinal thickness of zones 1, 2, and 3 were 9 to 16, 8 to 13, and 8 to 14 µm, respectively. Means and SDs for the asymmetry (when superior – inferior was used) for zones 1, 2, and 3 were 2 ± 5, 3 ± 6, and –2 ± 5 µm, respectively. The confidence intervals of SDs for the asymmetry of zones 1, 2, and 3 were 4 to 6, 5 to 8, and 4 to 7 µm, respectively. Between-subject variability of the asymmetry for the retinal thickness remained lower than that of the averaged retinal thickness across each zone ($F > 2.5$, $P < .01$). Asymmetry analysis indicated that one of the control participants had one zone flagged for asymmetry in the retinal thickness at $P < .01$, whereas none were flagged with two contiguous zones at $P < .05$. The asymmetry analysis of the retinal thickness flagged 16 of 20 patients we recruited. Three patients who were not flagged had global loss in the retinal thickness in the macula; one patient (patient 17) did not show macular damage.

Asymmetry Analysis of the Ganglion Cell Layer Thickness

Means ± SDs for the ganglion cell layer thickness in the age-similar control participants were as follows: 39 ± 4 µm for zone 1, 41 ± 3 µm for zone 2, and 37 ± 4 µm for zone 3. The confidence interval of SDs for the ganglion cell layer thickness of all three zones was 3 to 5 µm. Means and SDs for the asymmetry for zones 1, 2, and 3 were –1 ± 1, 1 ± 2, and –2 ± 2 µm, respectively. The confidence interval of SDs for the asymmetry of all three zones was

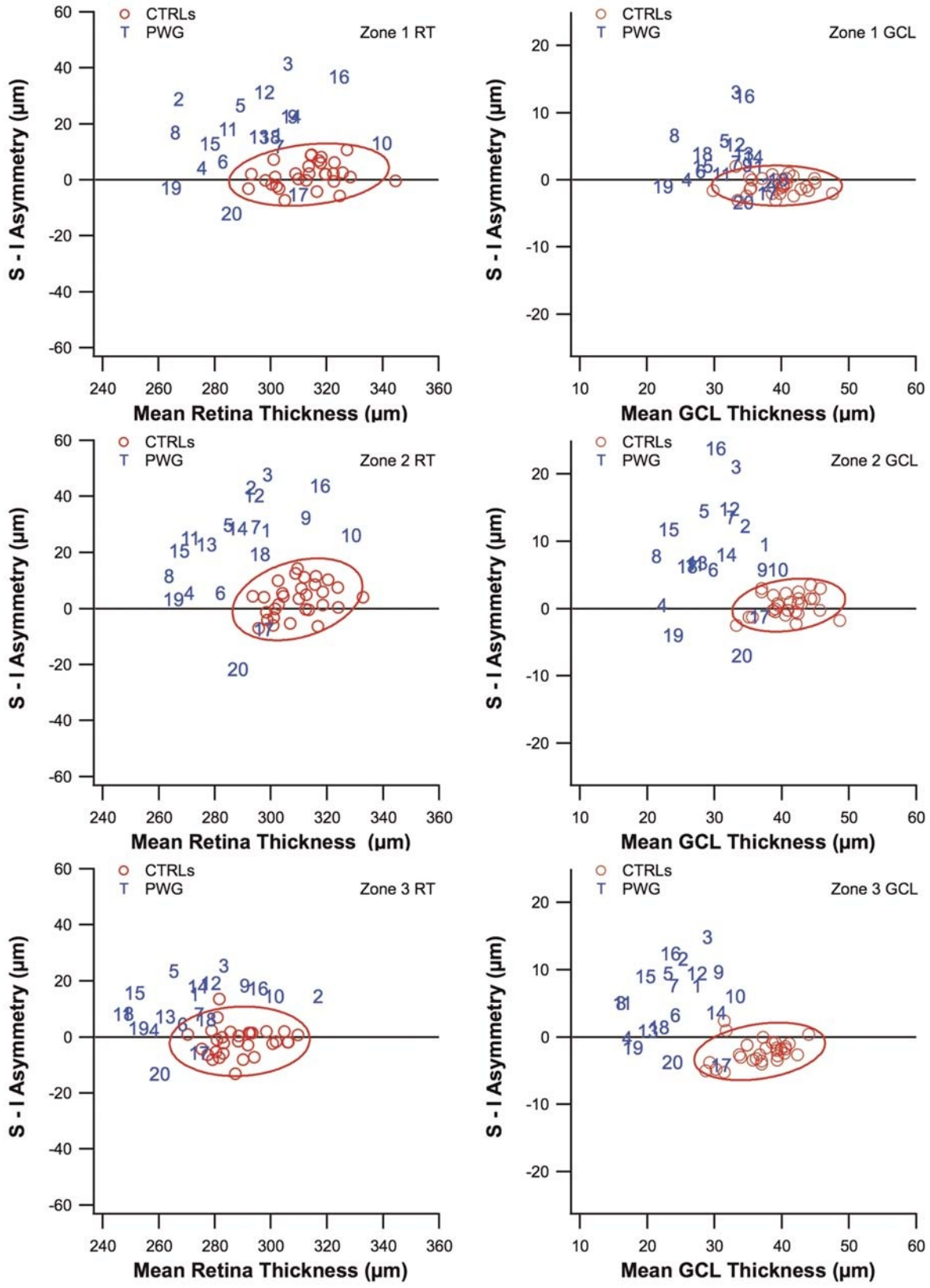

FIGURE 2. The asymmetry values (superior – inferior) on the *y* axis as a function of the mean retinal thickness (left column) and mean ganglion cell layer thickness (right column) for each zone that we established. Numbers represent the patient numbers, and the ellipses indicate the 95% reference range for zones 1, 2, and 3 as in Fig. 1. CTRLs = control participants; GCL = ganglion cell thickness; PWG = patients with glaucoma; RT = retinal thickness.

1 to 2 µm. We found that between-subject variability was significantly reduced when using the asymmetry of ganglion cell layer thickness as compared with the averaged ganglion cell layer thickness across each zone ($F > 4.5$, $P < .001$). The asymmetry of ganglion cell layer thickness flagged only one zone at $P < .05$ in two participants of the age-similar group. In addition to the 16 patients who were identified using the asymmetry of the retinal thickness, two more patients with glaucoma were identified using the asymmetry analysis of the ganglion cell layer thickness (at least two zones at $P < .05$ and/or at least one zone at $P < .01$). One of the remaining patients (patient 17) had a visual field defect at the far periphery, and the other patient (patient 4) had global loss of the ganglion cell layer thickness in which the ganglion cell layer thickness alone was flagged, as can be seen in Fig. 2.

Fig. 2 shows the asymmetry versus the mean thickness (of both retinal thickness and ganglion cell layer thickness) for each zone with 95% ellipses for the reference range derived from the age-similar control participants. There were four patients (patients 6, 7, 17, and 18) whose data fell within the 95% ellipse for zone 3 in the asymmetry of retinal thickness, whereas there were six patients (patients 1, 2, 10, 11, 17, and 20) whose data fell within the 95% ellipse for zone 1 in the asymmetry of ganglion cell layer thickness. For the other zones in both retinal thickness and ganglion cell layer thicknesses, there was one patient (patient 17) whose data fell within the 95% ellipse.

There were nine patients (patients 1, 2, 7, 9, 10, 14, 16, 17, and 18) whose data fell within the 95% ellipse for the mean of asymmetries across all zones for retinal thickness measurements (Fig. 3, left panel). However, there was only one patient (patient 17) whose data fell within the 95% ellipse for the mean asymmetries across all zones for ganglion cell layer thickness measurements, as can be seen in the right panel of Fig. 3.

Fig. 4 demonstrates two of three cases where the asymmetry analysis of the ganglion cell layer thickness identified abnormality (right panel), whereas the asymmetry of the retinal thickness (left panel) did not. Among the patients we tested, 16 patients were flagged using both the asymmetry of the retinal thickness and the ganglion cell layer thickness (Fig. 5). In 10 of these patients, there were an equal number of regions of abnormal asymmetry in both the retinal thickness and ganglion cell layer thickness measurements (Fig. 5). In three cases, there were more regions of abnormal asymmetry in ganglion cell layer thickness (Fig. 6; top row), whereas there were more regions of abnormal asymmetry in retinal thickness in the remaining three cases (Fig. 6; bottom row).

Fig. 7 demonstrates examples of four patients in which the pattern of the glaucomatous damage is shown on the en face images as dark areas (black arrows) representing the projection of the damaged retinal nerve fiber layer bundles. The patterns of glaucomatous damage were consistent with those found using the asymmetry analysis of the ganglion cell layer thickness as shown with the small plots at the bottom of each panel in Fig. 7. The gray scale of perimetric results as derived from the Humphrey field analyzer, in which darker areas indicate abnormal perimetric locations, was combined to illustrate comparison between structural and perimetric defect in regard to the extent of the glaucomatous damage.

DISCUSSION

It has been reported that there is high between-subject variability in the number of ganglion cells,[22–24] which poses a challenge in detecting structural loss due to glaucoma. We previously presented a method of analysis[20] to reduce the impact of this variability in control participants by using asymmetry analysis of the macular

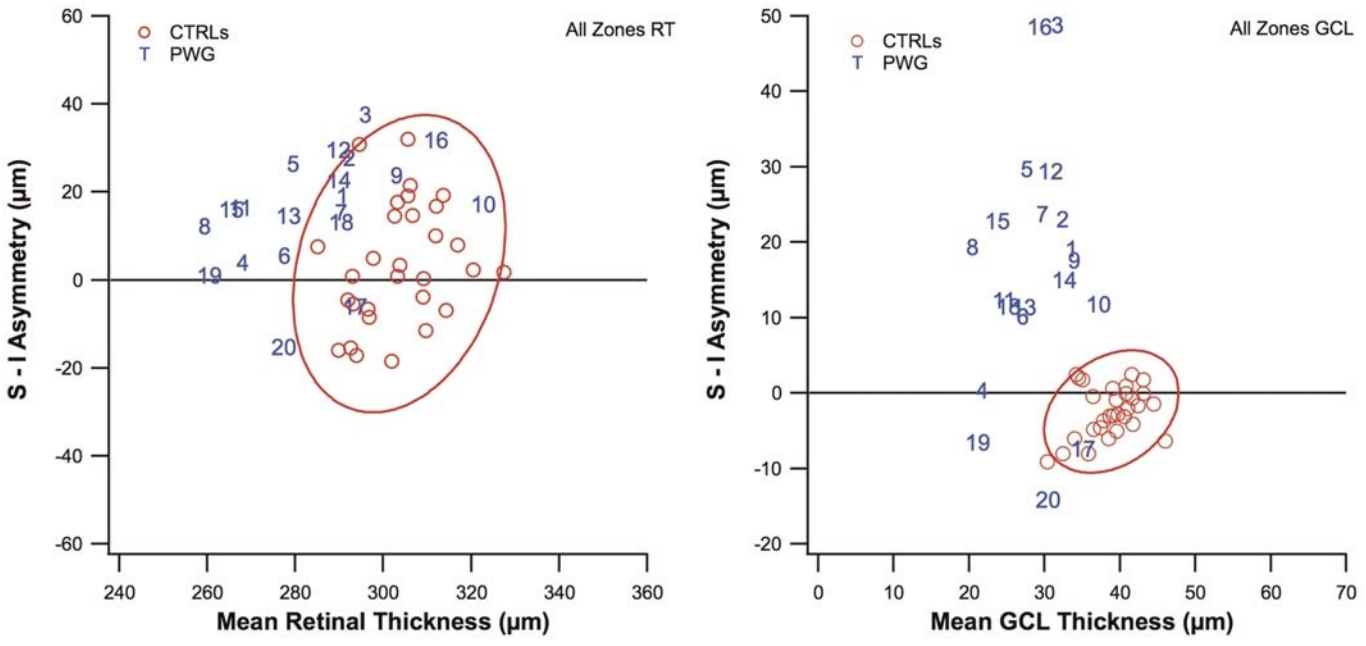

FIGURE 3. The mean of asymmetry values across all zones (superior – inferior) on the *y* axis as a function of mean thickness across all zones for retinal thickness (left panel) and for ganglion cell layer thickness (right panel). The ellipses indicate the 95% reference range. CTRLs = control participants; GCL = ganglion cell thickness; PWG = patients with glaucoma; RT = retinal thickness. It can be observed that the between-subject variability of asymmetry is lower for GCL thickness (right panel) than that for retinal thickness (left panel).

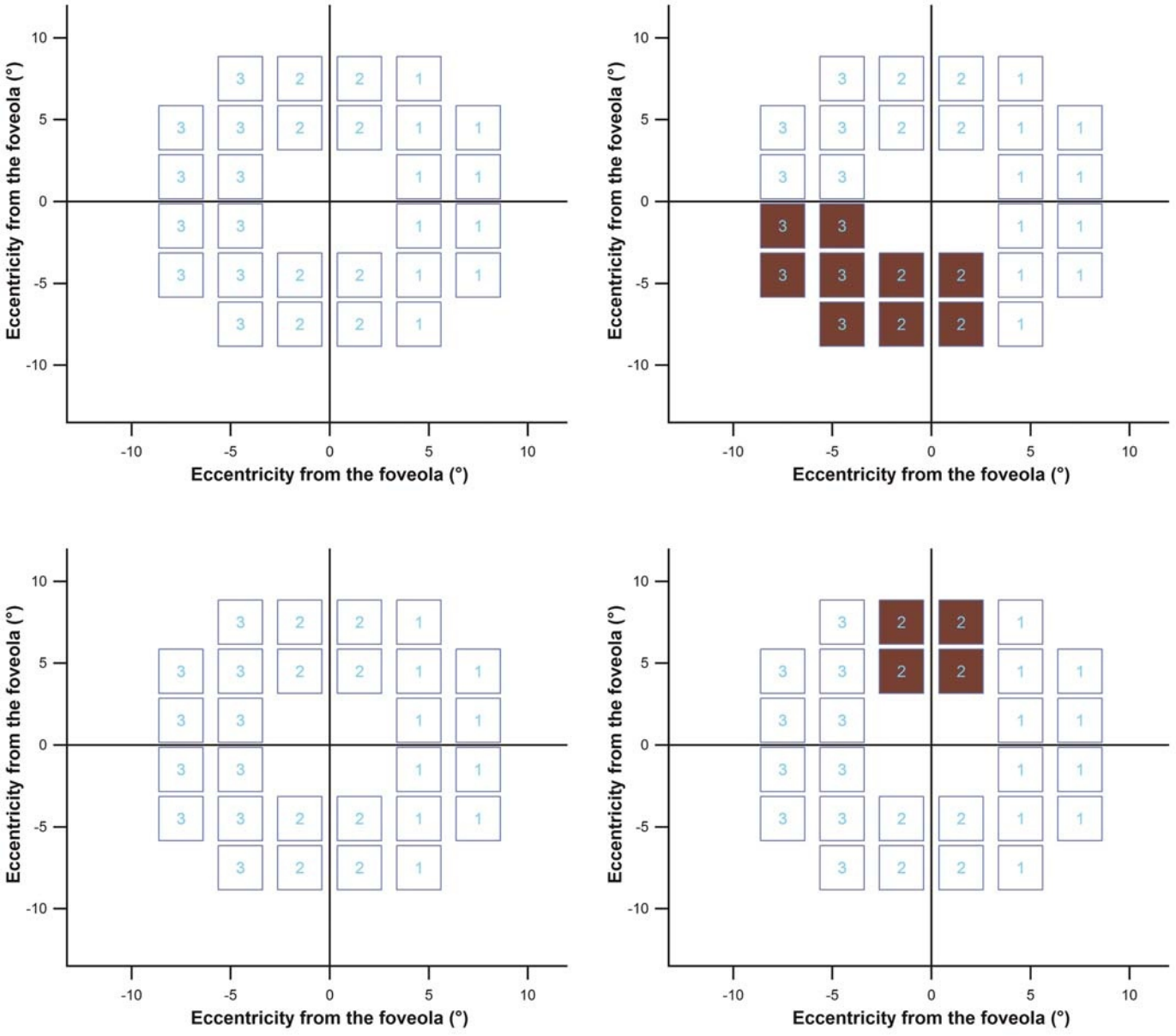

FIGURE 4. Examples of two patients with different results for the asymmetry of the retinal thickness (left column) and asymmetry of the ganglion cell layer (GCL) thickness (right column). The dark pink boxes represent that the asymmetry was beyond the 0.5th percentile. These two examples were derived from the two patients whose retinal thickness data did not identify reduction (left), whereas their GCL thickness data did (right). The number inside each box indicates the zone. The axes represent vertical (*y* axis) and horizontal (*x* axis) eccentricities.

thickness, a tool that has been used to assess structural loss to the macula. In the current study, we developed an approach based on clinical knowledge and the anatomy of the retinal nerve fiber layer bundles to provide better interpretation of the asymmetry analysis results in patients with glaucoma. We found evidence of structural damage to the macula in all patients with glaucoma, except one who had a visual field defect only at the far periphery.

The reduction of the between-subject variability that we found in the previous study was limited to 14 (seven each in superior and inferior hemifields) of the 64 boxes in the grid for the posterior pole. In an effort to improve the usefulness of the posterior pole asymmetry analysis, we increased the number of boxes in the analysis to 28 (within ±9° from the foveola in superior and inferior hemifields, Fig. 1) based on two considerations. First, we applied more clinically useful regions of the posterior pole grid when diagnosing patients with glaucoma, which are consistent with the projections of retinal nerve fiber layer bundles as reported in the literature on the retinal nerve fiber layer anatomy in humans[25,26] and in studies that traced bundles using scanning laser ophthalmoscopy images.[27–29] Second, we included regions that we found in the previous study[20] that had low between-subject variability. We additionally excluded regions where there were more and larger blood vessels than those in zones we chose, to reduce the likelihood of increased between-subject variability.

We verified that within-eye asymmetry analysis of these zones reduced between-subject variability in our normative data. We established

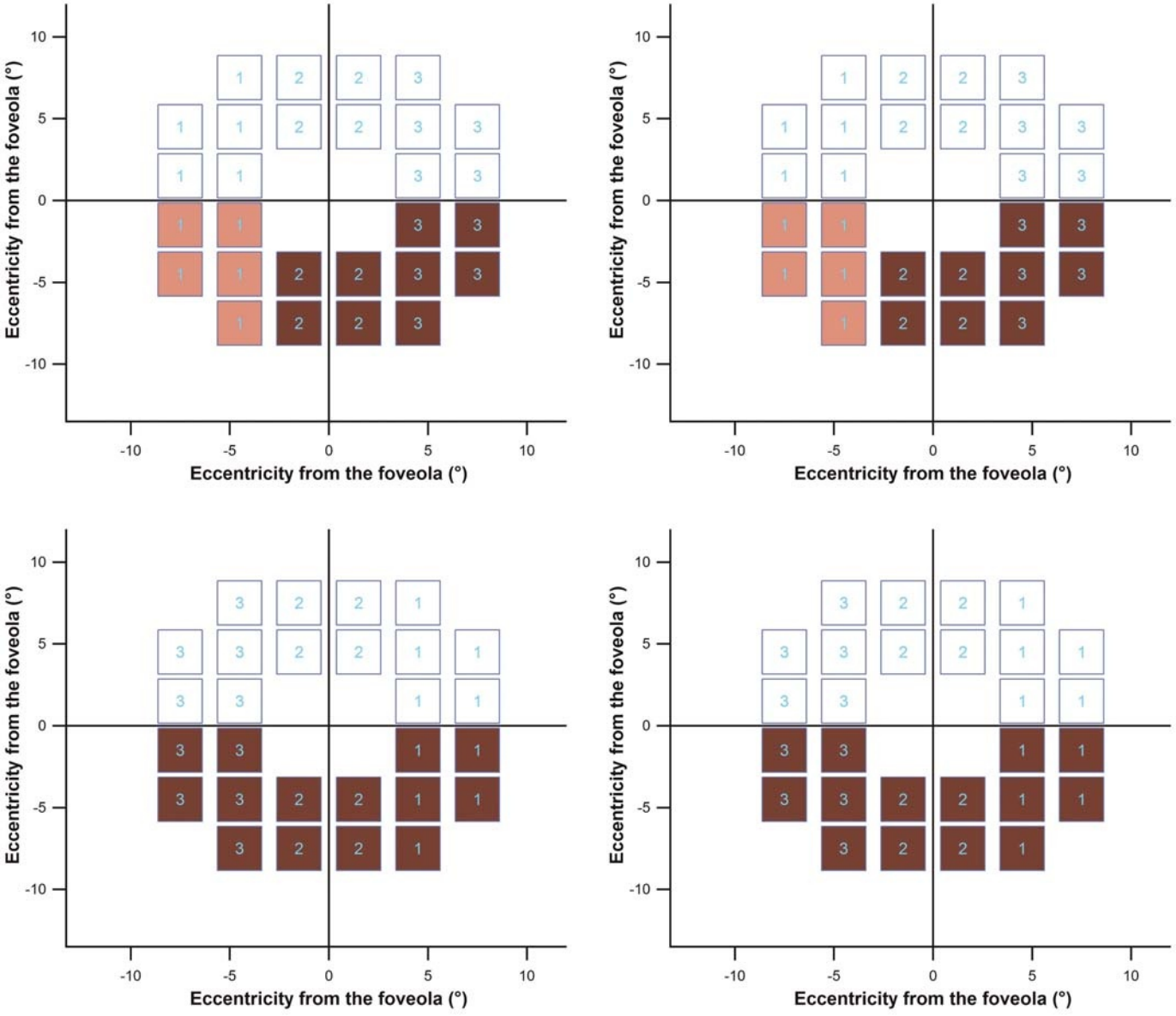

FIGURE 5. Examples of two patients with similar results of the asymmetry of the retinal thickness (left column) and asymmetry of the ganglion cell layer (GCL) thickness (right column). The light and dark pink boxes represent that the asymmetry was beyond the 2.5th and 0.5th percentiles, respectively.

normative data for the three zones and criteria for defining abnormality, because the printouts of the asymmetry from the Spectralis optical coherence tomograph had at least one "black box" (the most extreme degree of asymmetry analysis in the printout) for most control participants, which was also reported in a prior study.[30] In the current study, asymmetry analysis of the ganglion cell layer thickness flagged 18 of 20 patients using our criteria, and one additional patient had ganglion cell layer thinner than any of the age-similar control participants. Interestingly, the mean of asymmetries across all zones indicated stronger performance for the ganglion cell layer thicknesses than for the retinal thicknesses (Fig. 3).

We used en face optical coherence tomography images of retinal nerve fiber layer bundles to confirm the pattern of the thickness loss observed in both whole retinal thickness and ganglion cell layer thickness. The use of these images allowed us to visualize different depths of the retinal nerve fiber layer and to follow the patterns of the damaged retinal nerve fiber layer bundles on their way to the optic disc. As shown in Fig. 7, arcuate dark bands that represent the damage to the retinal nerve fiber layer bundles corresponded with glaucomatous loss found with the asymmetry analysis.

Another aspect of between-subject variation is the location of the temporal raphe. To estimate the impact of this aspect, we reanalyzed the data with the posterior pole grid oriented with the horizontal line, for boxes temporal to the fovea, while the nasal boxes remained oriented with the foveal-disc angle. The results were similar to those we found by applying the approach we used in the current study, which was orienting the posterior pole grid within the foveal-disc angle along the nasal and temporal sides to the fovea. This similarity may be because we limited the analysis to no more than 9° temporal to the fovea, corresponding to

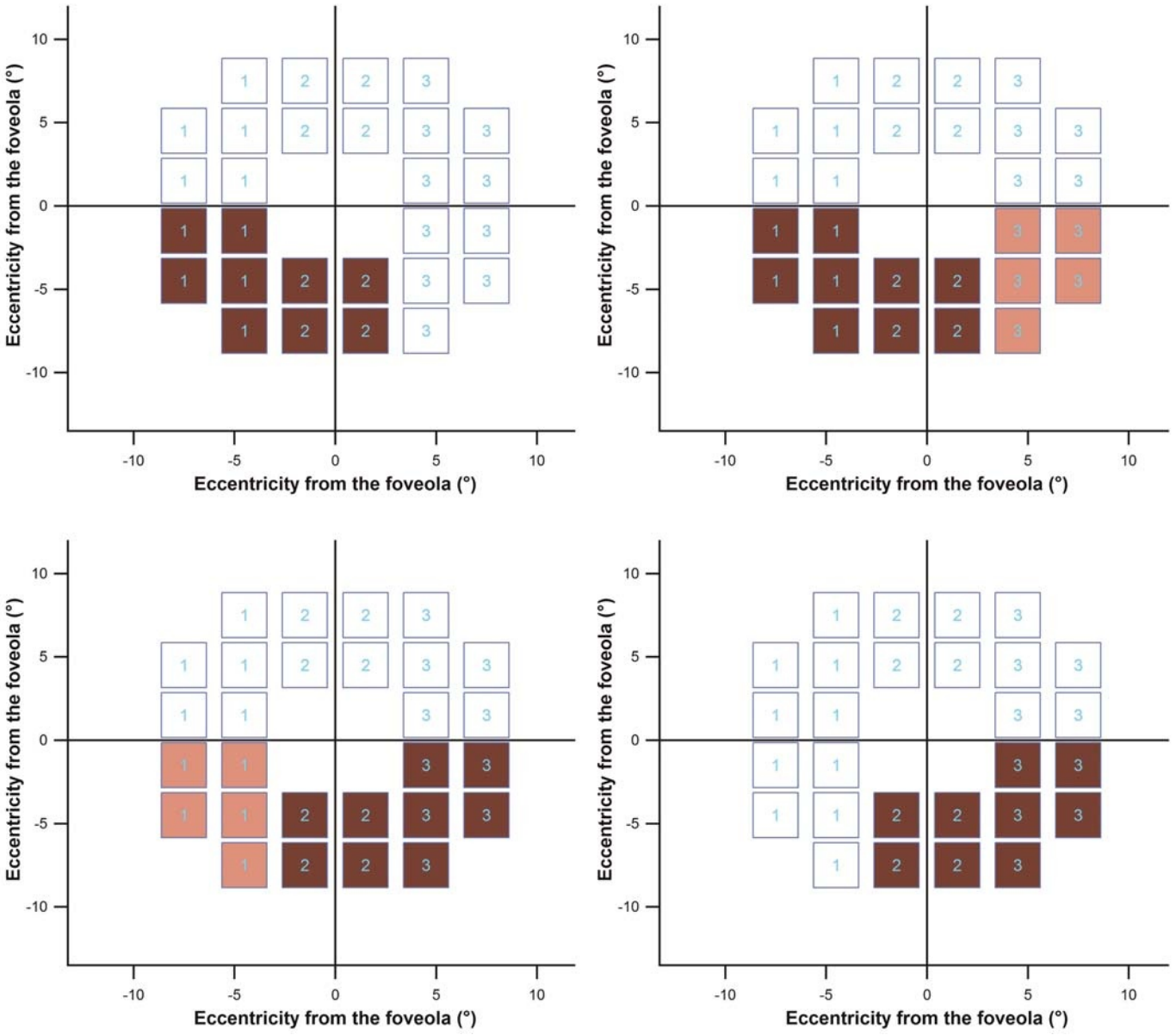

FIGURE 6. Examples of two patients with similar results, but with different extent of the retinal thickness asymmetry (left column) and ganglion cell layer (GCL) thickness asymmetry (right column). The light and dark pink boxes are as in Fig. 5. The top row shows an example of cases in which asymmetry of GCL thickness indicated greater extent of the damage than asymmetry of the retinal thickness, whereas the opposite results were found in some other cases as shown in the bottom row.

the vertical region of the temporal raphe as described by Vrabec.[25] The vertical region has been found to have a shallower angle than the triangular and oblique regions.[25,31] This reanalysis indicates that the region we included in our analysis had a small impact of between-subject variation in the angle of the temporal raphe.

In this study, the asymmetry analysis of the ganglion cell layer thickness seemed to be more sensitive to macular damage than that of the whole retinal thickness (Fig. 4). The asymmetry analysis of both retinal thickness and ganglion cell layer thickness demonstrated similar performance in 16 of 20 patients we recruited (Fig. 5). Fig. 6 shows examples of cases in which the asymmetry of ganglion cell layer thickness showed more affected areas than the asymmetry of the retinal thickness, whereas in other cases the opposite occurred (bottom row of Fig. 6).

Several studies focused on macular damage using the ganglion cell complex to assess reduction in thickness in patients with glaucoma. These studies showed that there was an association between the decrease of ganglion cell complex thickness and reduced visual field sensitivities using 10-2 grid in corresponding locations.[14,32–34] However, these studies had large between-subject variability for the ganglion cell complex measurements, which may reduce the ability to detect glaucomatous damage to the macula. In the current study, we were able to reduce the normal between-subject variability by using the autosegmentation of the ganglion cell layer with the Spectralis optical coherence tomograph and

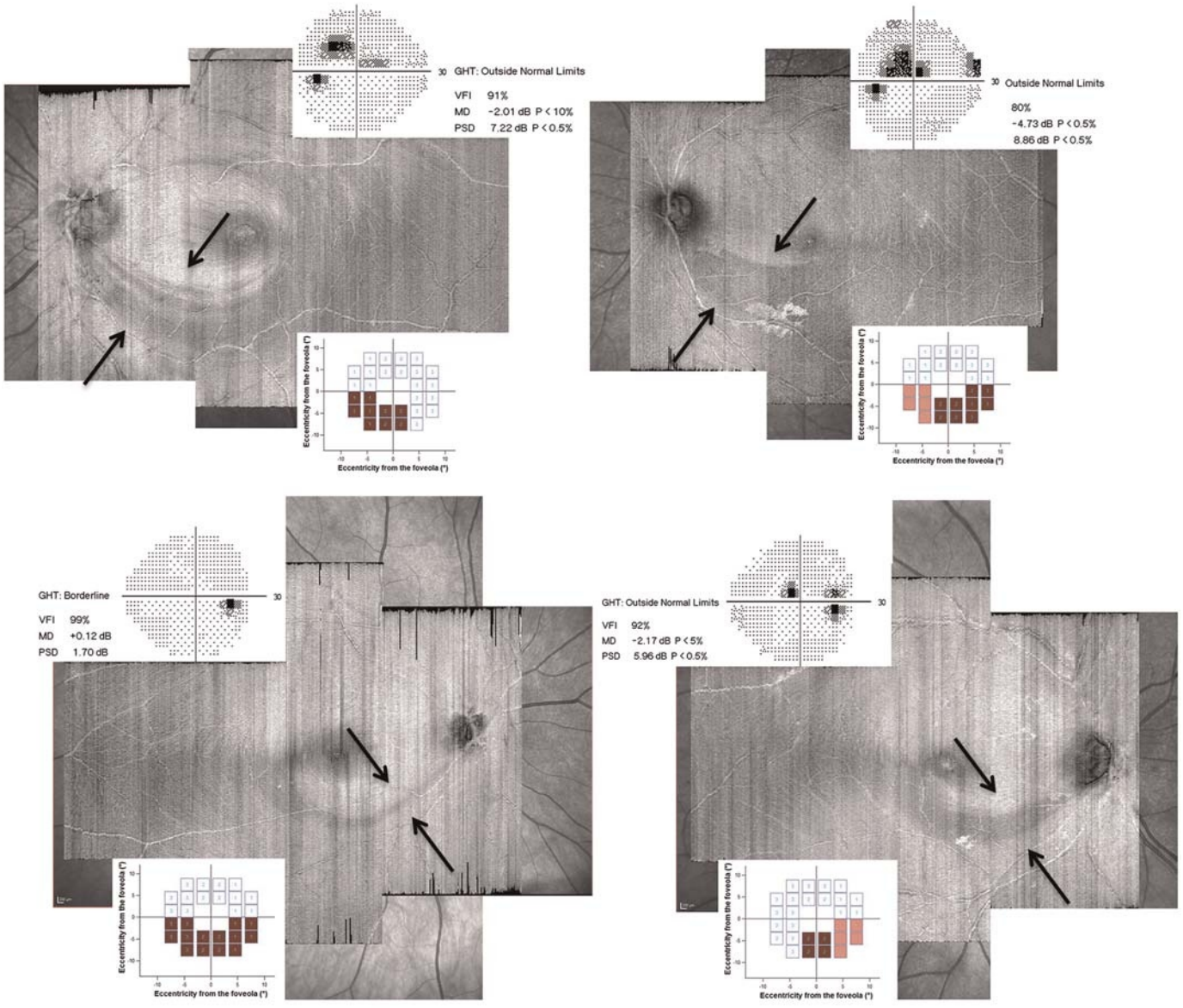

FIGURE 7. En face optical coherence tomography images that show patterns of glaucomatous damage to the retinal nerve fiber layer (RNFL) bundles as indicated by the dark areas (black arrows) in four examples. These patterns of damage were consistent with results from the asymmetry, which are demonstrated with small plots on the bottom of each en face image found by applying our zones and criteria. The upper plot of each en face image shows gray-scale printouts from the 24-2 testing pattern.

applying the new zones and criteria. These patients had been diagnosed with glaucoma as described in a previously published glaucoma study in which macular damage was not required to be present.[21]

Although asymmetry analysis identified most of the patients with glaucoma by using retinal thickness, as well as ganglion cell layer thickness, there were several limitations. First, the sample sizes were relatively small in this study in order to allow replication of the results. A second limitation was that, as reported from histological data, there is a substantial number of displaced amacrine cells in the ganglion cell layer.[22] This number increases as the eccentricity from the foveola increases, which would mainly affect the measurements for zone 3 of our new zones. Moreover, nonneural components such as blood vessels and glial tissues in both the whole retinal thickness and ganglion cell layer thickness could be confounders, and they should be considered when measuring the retinal thickness and ganglion cell layer thickness. This may decrease the level of the specificity of the test when it is applied in other studies because glial tissues, as an example of the nonneural components, may increase with age.[35] The last limitation was the potential of magnification effect on retinal thickness and ganglion cell layer thickness measurements caused by the variations in axial length and corneal curvature. The magnification factors should be considered because they affect the circumpapillary retinal nerve fiber layer measurements, although little effect was reported

in our previous study on retinal thickness measurements using the posterior pole asymmetry analysis.[20]

In conclusion, we found that, using our zones and criteria, glaucomatous damage to macular thickness was present in all but one of our patients with glaucoma. We focused on regions of the posterior pole of the asymmetry analysis because these regions are clinically relevant to the glaucomatous damage and followed the projections of the retinal nerve fiber layer bundles. We confirmed our results by using en face optical coherence tomography images to visualize the retinal nerve fiber layer bundles in a subset of our patients. These findings demonstrated the potential of using asymmetry analysis by applying our zones and criteria. Further investigations are warranted to validate the approach we developed in this study.

ARTICLE INFORMATION

Submitted: January 17, 2017

Accepted: September 17, 2017

Funding/Support: This work was supported by the US National Institutes of Health (grants NIH EY007716 and R01EY024542).

Conflict of Interest Disclosure: WHS is a consultant for Carl Zeiss Meditec and Heidelberg Engineering. MSA, VEM, and BJK have no conflicts of interest.

Author Contributions: Conceptualization: MSA, WHS, BJK; Data Curation: MSA, WHS, BJK; Formal Analysis: MSA, WHS; Investigation: MSA, WHS, BJK; Methodology: MSA, WHS, BJK; Visualization: MSA; Writing – Original Draft: MSA; Writing – Review & Editing: MSA, WHS, BJK; Funding Acquisition: WHS; Resources: WHS, BJK; Supervision: WHS, BJK.

REFERENCES

1. Blumberg DM, de Moraes CG, Prager AJ, et al. Association between Undetected 10-2 Visual Field Damage and Vision-related Quality of Life in Patients with Glaucoma. JAMA Ophthalmol 2017;135:742–7.

2. Anctil JL, Anderson DR. Early Foveal Involvement and Generalized Depression of the Visual Field in Glaucoma. Arch Ophthalmol 1984;102:363–70.

3. Stamper RL. The Effect of Glaucoma on Central Visual Function. Trans Am Ophthalmol Soc 1984;82:792–826.

4. King D, Drance SM, Douglas GR, et al. The Detection of Paracentral Scotomas with Varying Grids in Computed Perimetry. Arch Ophthalmol 1986;104:524–5.

5. Lachenmayr BJ, Drance SM. Diffuse Field Loss and Central Visual Function in Glaucoma. Ger J Ophthalmol 1992;1:67–73.

6. Zeimer RC, Mori MT, Khoobehi B. Feasibility Test of a New Method to Measure Retinal Thickness Noninvasively. Invest Ophthalmol Vis Sci 1989;30:2099–105.

7. Zeimer R, Shahidi M, Mori M, et al. A New Method for Rapid Mapping of the Retinal Thickness at the Posterior Pole. Invest Ophthalmol Vis Sci 1996;37:1994–2001.

8. Zeimer R, Asrani S, Zou S, et al. Quantitative Detection of Glaucomatous Damage at the Posterior Pole by Retinal Thickness Mapping. A Pilot Study. Ophthalmology 1998;105:224–31.

9. Asrani S, Zou S, d'Anna S, et al. Noninvasive Mapping of the Normal Retinal Thickness at the Posterior Pole. Ophthalmology 1999;106:269–73.

10. Greenfield DS, Bagga H, Knighton RW. Macular Thickness Changes in Glaucomatous Optic Neuropathy Detected Using Optical Coherence Tomography. Arch Ophthalmol 2003;121:41–6.

11. Bagga H, Greenfield DS, Knighton RW. Macular Symmetry Testing for Glaucoma Detection. J Glaucoma 2005;14:358–63.

12. Kanadani FN, Hood DC, Grippo TM, et al. Structural and Functional Assessment of the Macular Region in Patients with Glaucoma. Br J Ophthalmol 2006;90:1393–7.

13. Wang M, Hood DC, Cho JS, et al. Measurement of Local Retinal Ganglion Cell Layer Thickness in Patients with Glaucoma Using Frequency-domain Optical Coherence Tomography. Arch Ophthalmol 2009;127:875–81.

14. Raza AS, Cho J, de Moraes CG, et al. Retinal Ganglion Cell Layer Thickness and Local Visual Field Sensitivity in Glaucoma. Arch Ophthalmol 2011;129:1529–36.

15. Hood DC, Raza AS, de Moraes CG, et al. Glaucomatous Damage of the Macula. Prog Retin Eye Res 2013;32:1–21.

16. Raza AS, Zhang X, de Moraes CG, et al. Improving Glaucoma Detection Using Spatially Correspondent Clusters of Damage and by Combining Standard Automated Perimetry and Optical Coherence Tomography. Invest Ophthalmol Vis Sci 2014;55:612–24.

17. Kim HJ, Lee SY, Park KH, et al. Glaucoma Diagnostic Ability of Layer-by-layer Segmented Ganglion Cell Complex by Spectral-domain Optical Coherence Tomography. Invest Ophthalmol Vis Sci 2016;57:4799–805.

18. Asrani S, Rosdahl JA, Allingham RR. Novel Software Strategy for Glaucoma Diagnosis: Asymmetry Analysis of Retinal Thickness. Arch Ophthalmol 2011;129:1205–11.

19. Um TW, Sung KR, Wollstein G, et al. Asymmetry in Hemifield Macular Thickness as an Early Indicator of Glaucomatous Change. Invest Ophthalmol Vis Sci 2012;53:1139–44.

20. Alluwimi MS, Swanson WH, Malinovsky VE. Between-subject Variability in Asymmetry Analysis of Macular Thickness. Optom Vis Sci 2014;91:484–90.

21. Swanson WH, Malinovsky VE, Dul MW, et al. Contrast Sensitivity Perimetry and Clinical Measures of Glaucomatous Damage. Optom Vis Sci 2014;91:1302–11.

22. Curcio CA, Allen KA. Topography of Ganglion Cells in Human Retina. J Comp Neurol 1990;300:5–25.

23. Blanks JC, Torigoe Y, Hinton DR, et al. Retinal Pathology in Alzheimer's Disease. I. Ganglion Cell Loss in Foveal/Parafoveal Retina. Neurobiol Aging 1996;17:377–84.

24. Provis JM, van Driel D, Billson FA, et al. Development of the Human Retina: Patterns of Cell Distribution and Redistribution in the Ganglion Cell Layer. J Comp Neurol 1985;233:429–51.

25. Vrabec F. The Temporal Raphe of the Human Retina. Am J Ophthalmol 1966;62:926–38.

26. Fitzgibbon T, Taylor SF. Retinotopy of the Human Retinal Nerve Fibre Layer and Optic Nerve Head. J Comp Neurol 1996;375:238–51.

27. Airaksinen PJ, Doro S, Veijola J. Conformal Geometry of the Retinal Nerve Fiber Layer. Proc Natl Acad Sci U S A 2008;105:19690–5.

28. Jansonius NM, Schiefer J, Nevalainen J, et al. A Mathematical Model for Describing the Retinal Nerve Fiber Bundle Trajectories in the Human Eye: Average Course, Variability, and Influence of Refraction, Optic Disc Size and Optic Disc Position. Exp Eye Res 2012;105:70–8.

29. Denniss J, Turpin A, Tanabe F, et al. Structure-function Mapping: Variability and Conviction in Tracing Retinal Nerve Fiber Bundles and Comparison to a Computational Model. Invest Ophthalmol Vis Sci 2014;55:728–36.

30. Seo JH, Kim TW, Weinreb RN, et al. Detection of Localized Retinal Nerve Fiber Layer Defects with Posterior Pole Asymmetry Analysis of Spectral Domain Optical Coherence Tomography. Invest Ophthalmol Vis Sci 2012;53:4347–53.

31. Huang G, Gast TJ, Burns SA. In Vivo Adaptive Optics Imaging of the Temporal Raphe and Its Relationship to the Optic Disc and Fovea in the Human Retina. Invest Ophthalmol Vis Sci 2014;55:5952–61.

32. Hood DC, Raza AS, de Moraes CG, et al. Initial Arcuate Defects within the Central 10 Degrees in Glaucoma. Invest Ophthalmol Vis Sci 2011;52:940–6.

33. Le PV, Tan O, Chopra V, et al. Regional Correlation among Ganglion Cell Complex, Nerve Fiber Layer, and Visual Field Loss in Glaucoma. Invest Ophthalmol Vis Sci 2013;54:4287–95.

34. Miraftabi A, Amini N, Morales E, et al. Macular SD-OCT Outcome Measures: Comparison of Local Structure-function Relationships and Dynamic Range. Invest Ophthalmol Vis Sci 2016;57:4815–23.

35. Harwerth RS, Wheat JL, Rangaswamy NV. Age-related Losses of Retinal Ganglion Cells and Axons. Invest Ophthalmol Vis Sci 2008;49:4437–43.